

ORFEUS observations of S VI, O VI and P V in the stellar wind from the nucleus of NGC 6543

J. Zweigle¹, M. Grewing^{1,2}, J. Barnstedt², M. Götz², W. Gringel², C. Haas², W. Hopfensitz², N. Kappelmann², G. Krämer², I. Appenzeller³, J. Krautter³, and H. Mandel³

¹ Institut de Radio Astronomie Millimétrique (IRAM), 300 Rue de la Piscine, F-38406 Saint Martin d'Hères, France

² Institut für Astronomie und Astrophysik der Universität Tübingen, Waldhäuserstr. 64, D-72076 Tübingen, Germany

³ Landessternwarte Heidelberg-Königstuhl, Königstuhl 12, D-69117 Heidelberg, Germany

Received 22 August 1996 / Accepted 20 November 1996

Abstract. During the ORFEUS-SPAS (Orbiting Retrievable Far and Extreme Ultraviolet Spectrometer on the Shuttle Pallet Satellite) mission STS-51, flown in September 1993, we observed, to our knowledge for the first time, the central star of the planetary nebula NGC 6543 in the far ultraviolet (90 nm - 115 nm) wavelength region using the University of California, Berkeley spectrometer. The spectral resolution of the instrument during the flight was about 0.03 nm.

The observed stellar continuum energy distribution can be approximated by a modelled stellar atmosphere from Clegg and Middlemass with a temperature of 50 000 K and a gravity of $\log(g)=4.5$, using an extinction of $E(B-V)=0.08$.

In addition to narrow absorption lines of atomic species (e.g. H I, C I, N I, O I) the spectrum shows narrow absorption lines of molecular hydrogen and strong P-Cygni line profiles of the S VI (93.3 nm, 94.5 nm), O VI (103.2 nm, 103.8 nm) and P V (111.8 nm, 112.8 nm) resonance doublets. The analysis of these three P-Cygni line doublets using the escape probability method yields together with the consideration of the N V (123.9 nm, 124.3 nm), Si IV (139.4 nm, 140.3 nm) and C IV (154.8 nm, 155.1 nm) P-Cygni line doublets from IUE spectra as a mean value for the lower limit of the central star's mass loss rate $2.8 \cdot 10^{-9} M_{\odot}/\text{yr}$. This value for the stellar mass loss rate of the nucleus of NGC 6543 is compatible within a factor of two with the expected mass loss rate from the approximate radiation driven wind theory for an evolved star with a mass of $0.62 M_{\odot}$, a luminosity of $3\,030 L_{\odot}$ and an effective temperature of 50 000 K.

Key words: stars: individual – mass loss – spectroscopy – ultraviolet radiation – planetary nebulae

1. Introduction

The planetary nebula NGC 6543 (PN G096.4+29.9) with coordinates $\alpha_{2000} = 17^{\text{h}}58^{\text{m}}33^{\text{s}}$ and $\delta_{2000} = +66^{\circ}37'59''$ is one

Send offprint requests to: J. Zweigle

of the most complex planetary nebulae known. HST-WFPC 2 narrow-band-filter images (Harrington & Borkowski 1994) clarified its geometrical structure and revealed a wealth of new details. NGC 6543 exhibits helical structures, a complex velocity field with a high velocity jet (Miranda & Solf 1992), both with a high degree of point symmetry, and fast low ionization emission regions (Balick et al. 1994). This nebula is also known to show a ring-like distribution of x-ray emission (Kreysing et al. 1992). Its hydrogen rich central star is of spectral type Of/WR (Mendez et al. 1990).

Nuclei of planetary nebulae are strongly interacting with the nebular shell(s) surrounding them both through their ionizing photon flux and strong stellar winds. Different authors have studied extensively the wind from the nucleus of NGC 6543 in the wavelength region longward of $\text{Ly}\alpha$ by analysing low and high resolution spectra of the central star obtained with the short-wavelength camera of the IUE-satellite. Their results are summarized in table 1. Patriarchi and Perinotto (1995) reexamined all the high resolution spectra of central stars of PNe obtained so far with the short-wavelength camera of the IUE-satellite for variability in their P-Cygni line profiles and suggested a photometric variability in the central star of NGC 6543.

The spectral region between the Lyman limit at 91.2 nm and the $\text{Ly}\alpha$ line has been observed so far for only a few central stars of planetary nebulae at low resolution with the Ultraviolet Spectrometer aboard the Voyager probe (Polidan & Holberg 1985) and at moderate resolution with the Hopkins Ultraviolet Telescope (Bowers et al. 1995). This little-explored wavelength region is of great astrophysically interest, since it contains numerous atomic and ionic resonance lines and in addition the Lyman and Werner bands of molecular hydrogen. Of particular relevance is the O VI doublet (103.2 nm, 103.8 nm), which traces hotter portions of the stellar wind than any other line in the ultraviolet.

In the following we report an observation of the central star of NGC 6543 in the wavelength range between 90 nm and

Table 1. Stellar wind parameters of NGC 6543 derived by different authors. The table summarizes the types of IUE-spectra used: LRS (low resolution spectra) or HRS (high resolution spectra), the terminal velocities, the mass loss rates, the methods used for calculating the mass loss rates, and the corresponding references.

IUE-spectra	v_∞ [km/s]	\dot{M} [M_\odot /yr]	method	reference
LRS	2150	$1.0 \cdot 10^{-7}$	moments	Castor et al. (1981)
LRS	-	$1.7 \cdot 10^{-6}$	first order moments	Hutsemékers and Surdej (1987)
LRS	-	$1.4 \cdot 10^{-7}$	first order moments	Hutsemékers and Surdej (1989)
HRS	1900	$3.2 \cdot 10^{-7}$	escape probability	Bianchi et al. (1986)
HRS	1900	$4.0 \cdot 10^{-8}$	Sobolev with exact integration	Perinotto et al. (1989)

115 nm obtained with the ORFEUS telescope during the Space Shuttle mission STS-51 in September 1993.

2. Observation and data reduction

The central star of NGC 6543 was observed with the Berkeley spectrometer of the ORFEUS telescope on day 261 in 1993 from 17:47:53 UT to 18:14:04 UT with an effective exposure time of 1381 s. The ORFEUS telescope was mounted on the free-flying ASTRO-SPAS platform, which was deployed from and later recovered by the Space Shuttle DISCOVERY during the STS-51 mission in September 1993. The ORFEUS telescope contains a normal incidence parabolic primary mirror with a diameter of 100 cm that feeds the Berkeley spectrometer in the prime focus. The Berkeley spectrometer covers the wavelength band from 39 nm to 117 nm, utilising first order dispersion from four spherical varied line-spaced diffraction gratings simultaneously and two photon counting detectors equipped with curved microchannel plates and delay line anode readout systems (Hurwitz & Bowyer 1991). The in-flight spectral resolution of the Berkeley instrument (effective area about 4 cm²) for point sources corresponds to approximately $\lambda/\Delta\lambda = 3000$ (Hurwitz & Bowyer 1995). The wavelength scale carries an uncertainty of about 110 km/s caused by the unknown location of the target within the 20'' diameter circular focal plane aperture (Hurwitz & Bowyer 1996). The pointing stability during the observation was better than 2''.

The raw data were converted to FITS file format for reduction and processing of the spectra. Corrections were applied to remove background counts and scattered light. The flux calibration of the ORFEUS spectra is based on a comparison of the observed spectrum of the hot DA white dwarf G 191–B2b with a model spectrum and its error is smaller than 10% (Raymond et al. 1995). The wavelength scale of the spectra was improved using known positions of narrow molecular hydrogen absorption lines in the spectrum of the white dwarf BD+28 4211, also observed by ORFEUS during the STS–51 mission (Gölz, private communication).

Due to the high column density of interstellar hydrogen to NGC 6543 ($\log(N_{\text{H}}) = 20.62 - 20.71$, Fruscione et al. 1995), which implies a very large optical depth in the Lyman continuum region, only the spectral range between 91.2 nm and 115 nm is useful for the analysis of the central star of NGC 6543. Fig. 1 shows the observed spectrum in the wavelength range from 90 nm to 115 nm. It consists of a stellar continuum extending up

to the Lyman edge, where the flux drops to zero, with P-Cygni-type line profiles of S VI (93.3 nm, 94.5 nm), N IV (95.5 nm), C III (97.7 nm), N III (99 nm), O VI (103.2 nm, 103.8 nm) and P V (111.8 nm, 112.8 nm) superimposed. Moreover, sharp absorption lines of atomic hydrogen, other atomic and ionic species and the molecular hydrogen Lyman and Werner bands are visible against the continuum of the central star. In order to measure the wavelength centroids of absorption lines, we fit the local continuum with a low order polynomial and the absorption line profiles assuming Gaussian profiles. The measured central wavelengths of the absorption features were compared with literature data of interstellar line parameters (Morton 1991). Table 2 lists the resulting line identifications. We have included in this table only those lines where the measured wavelengths coincide within one spectral resolution element of 0.03 nm with the expected position of an absorption line.

The identified molecular hydrogen absorption lines can be explained by pure interstellar absorption, if the column density of molecular hydrogen in the direction of NGC 6543 is greater than about 10^{16} cm⁻². Savage et al. (1977) found from COPERNICUS observations of more than 100 stars an empirical relation between the fractional abundance of H₂ and the total hydrogen column density. Their results imply a molecular hydrogen column density greater than $2.2 \cdot 10^{16}$ cm⁻² for the total interstellar hydrogen density quoted above. We therefore conclude that the observed molecular hydrogen lines are of interstellar origin.

In the following we restrict ourselves to the analysis and discussion of the stellar continuum energy distribution and the stellar wind profiles.

3. Analysis and discussion

3.1. The stellar continuum

Since the nebular continuum contribution to the stellar continuum flux is decreasing with decreasing wavelength and since Bianchi et al. (1986) state that the nebular continuum contribution to the stellar continuum flux is less than 10% in the IUE-range, we neglect in the following discussion the nebular component of the continuum. Using an extinction $E(B - V)$ of 0.08 (Bianchi et al. 1986), we have compared the observed stellar continuum with reddened Clegg and Middlemass (1987) NLTE model atmospheres. In order to have a larger wavelength range for a more accurate determination of the effective temperature of the central star, we combined our ORFEUS data with

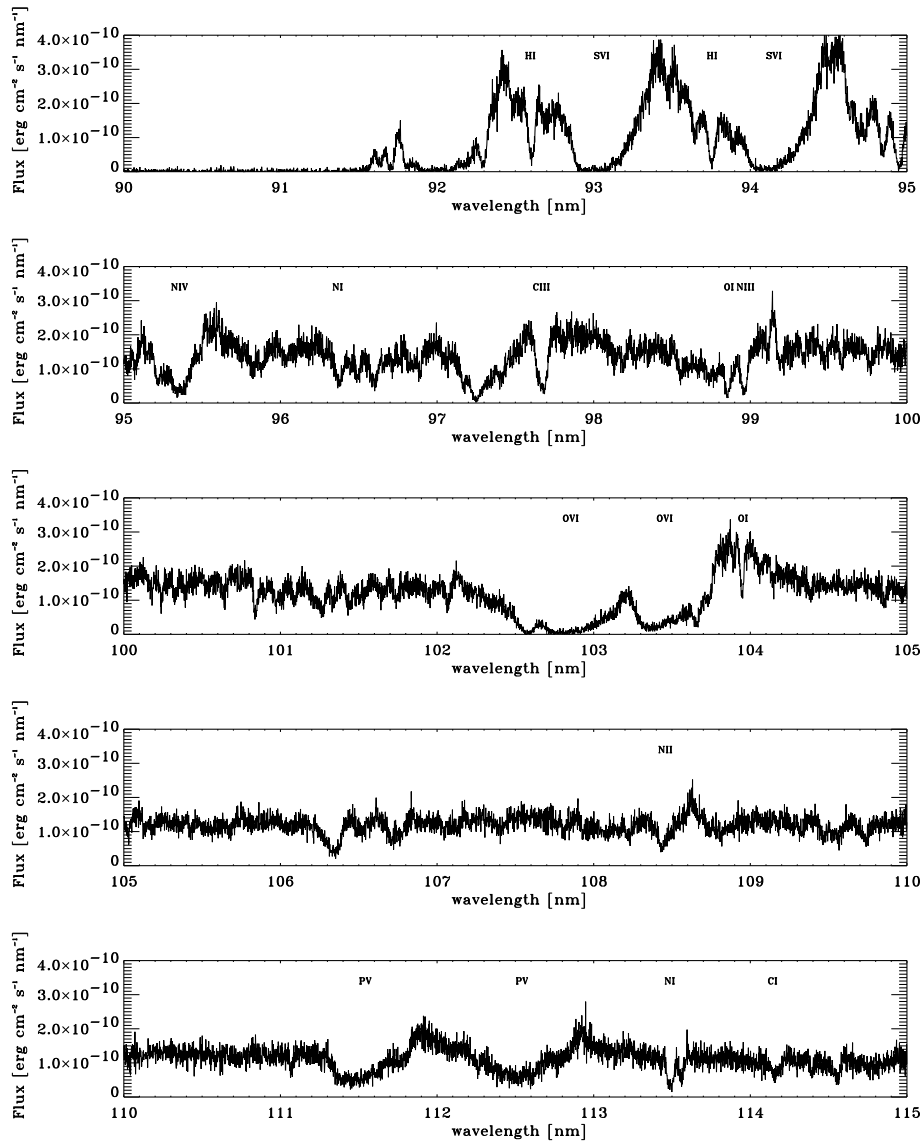


Fig. 1. Far ultraviolet spectrum of the central star of NGC 6543 in the wavelength region from 90 nm to 115 nm observed by ORFEUS.

low dispersion IUE data taken from the uniform low dispersion archive (ULDA). For the reddening of the model atmospheres in the far ultraviolet we extrapolated the extinction curve from Seaton (1979) down to 90 nm. The stellar flux distribution can then be well approximated by a model stellar atmosphere from Clegg and Middlemass (1987) with a temperature of 50 000 K and a gravity of $\log(g)=4.5$ (Fig. 2).

If one uses instead of the extrapolated extinction curve from Seaton (1979) an extrapolation of the extinction curve from Savage and Mathis (1979) one gets a dereddened observed continuum flux which is at the most 5% higher at the shortest wavelengths. But the temperature of the central star determined by the best fit of the model atmospheres to the observations remains almost unchanged, because it is mainly determined by the slope of the decline of the observed continuum flux longwards of 125 nm. The values in the literature for the central star's temperature scatter between 36 200 K (Natta et al. 1980) and 80 000 K (Bianchi et al. 1986) with an accumulation around

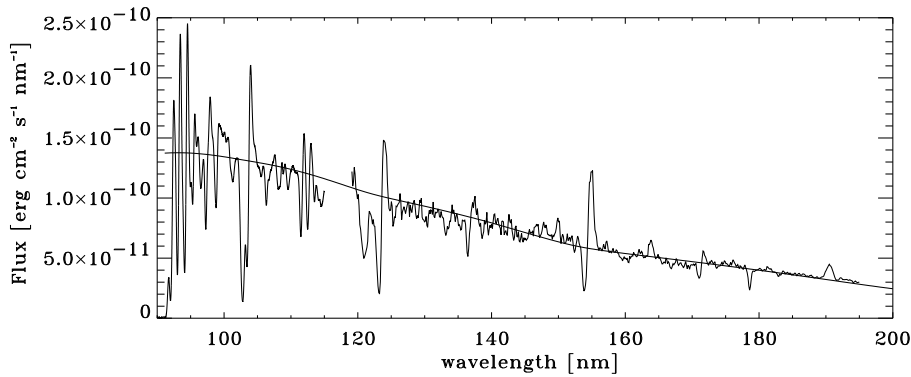
50 000 K. From the scaling of the model flux to the observed flux one gets

$$R_*/D = 1.26 \cdot 10^{-11}$$

where R_* is the stellar radius and D the distance of NGC 6543 in the same units. Since most central stars of planetary nebulae have masses of about $0.62 M_\odot$ (Górny et al. 1996) we assume further on that the mass of the nucleus is $0.62 M_\odot$. The value of $\log(g) = 4.5$ can then be converted into a stellar radius of $0.73 R_\odot$. From the comparison of the observed energy distribution with model atmospheres having different gravities we estimate that the stellar radius is uncertain by a factor of two. Since the value of $0.73 R_\odot$ for the stellar radius of the central star of NGC 6543 agrees well with other values (between $0.64 R_\odot$ and $0.8 R_\odot$) given by different authors (Castor et al. 1981, Bianchi et al. 1986 and Perinotto et al. 1989), we will use this value in the following. Inserting $R_* = 0.73 R_\odot$ in the equation above leads to a distance estimate for NGC 6543 of 1310 pc

Table 2. Line identifications for the narrow absorption lines in the ORFEUS spectrum of the central star of NGC 6543.

Species	λ_{obs} [nm]	λ_{lab} [nm]	Species	λ_{obs} [nm]	λ_{lab} [nm]	Species	λ_{obs} [nm]	λ_{lab} [nm]
HI	91.651	91.643	H ₂	97.489	97.488	HI	102.558	102.572
HI	91.721	91.719	H ₂	98.198	98.195	CII	103.641	103.634
HI	92.300	92.315	H ₂	98.562	98.563	CII	103.714	103.702
HI	92.613	92.623	OI	98.857	98.858	OI	103.931	103.923
H ₂	93.479	93.476	NIII	98.963	98.980	H ₂	104.129	104.116
OI	93.664	93.663	H ₂	99.194	99.202	H ₂	104.364	104.350
HI	93.770	93.780	H ₂	99.346	99.355	ArI	104.834	104.822
OI	93.912	93.923	H ₂	99.479	99.488	H ₂	105.005	104.996
H ₂	94.751	94.752	H ₂	99.585	99.598	H ₂	106.300	106.288
OI	94.871	94.868	H ₂	99.770	99.783	H ₂	106.493	106.500
HI	94.972	94.974	H ₂	100.175	100.183	H ₂	106.682	106.690
H ₂	95.046	95.040	H ₂	100.240	100.246	H ₂	107.014	107.014
OI	95.092	95.088	H ₂	100.323	100.330	H ₂	107.774	107.770
NI	95.240	95.242	H ₂	100.636	100.642	NII	108.447	108.456
NI	95.364	95.365	H ₂	100.839	100.839	H ₂	109.424	109.424
NI	96.396	96.399	H ₂	100.968	100.972	CII	109.730	109.737
NI	96.512	96.504	H ₂	101.083	101.094	CI	111.018	111.017
H ₂	96.622	96.627	H ₂	101.263	101.268	NI	113.429	113.417
H ₂	96.908	96.909	H ₂	101.332	101.343	NI	113.498	113.498
OI	97.184	97.174	H ₂	101.433	101.425	CI	114.086	114.071
HI	97.263	97.254	H ₂	101.733	101.743	CII	114.553	114.539
H ₂	97.419	97.416	SiII	102.060	102.070			

**Fig. 2.** Comparison of the ORFEUS spectrum (90 nm to 115 nm) combined with low dispersion IUE data (118 nm to 195 nm) of NGC 6543 with the best fit model stellar atmosphere from Clegg and Middlemass ($T_{\star} = 50\,000$ K and $\log(g) = 4.5$). The ORFEUS spectrum was degraded to the resolution of the IUE satellite in the low dispersion mode using a Gaussian profile having a full width at half maximum of 0.6 nm.

with an uncertainty of a factor of two. The statements for the distance of NGC 6543 in the literature reach from 0.55 kpc to 4.14 kpc (Acker et al. 1992).

3.2. The stellar wind

The spectral resolution of about 100 km/s in the ORFEUS spectrum of the nucleus of NGC 6543 allows to fit the P-Cygni line profiles arising in the expanding atmosphere of the central star with theoretical line profiles in order to compute the stellar mass loss rate. This technique was applied to the S VI (93.3 nm, 94.4 nm), O VI (103.2 nm, 103.8 nm) and P V (111.8 nm, 112.8 nm) lines. Theoretical profiles were calculated with the method of Olson (1982), improved by Bianchi et al. (1986). The trapping and escape coefficients are calculated by the escape probability method using the Sobolev approximation, which allows to compute profiles of close resonance line

doublets. The resulting best fits are shown in Fig. 3 for the three wind doublets mentioned above.

For all lines the velocity law assumed was

$$w(x) = w_0 + (1 - w_0)(1 - 1/x)^2$$

with the notation $x = r/R_{\star}$ and $w = v/v_{\infty}$. R_{\star} denotes the photospheric stellar radius, r the distance to the center, v_{∞} the terminal wind velocity, and w_0 the normalized velocity at the base of the stellar atmosphere. We used $w_0 = w(x=1) = 0.01$. As optical depth law we assumed

$$\tau(w) = \tau_{\text{tot}}(\gamma + 1)(1 - w_0)^{-1-\gamma}(1 - w)^{\gamma}$$

with a parameter γ and the total optical depth $\tau_{\text{tot}} = \int_{w_0}^1 \tau(w)dw$. The different parameters of the adopted theoretical profiles (figure 3) are compiled in table 3 together with the results given by Bianchi et al. (1986) for the P-Cygni line profiles of NV (123.9 nm, 124.3 nm), Si IV (139.4 nm, 140.3 nm) and CIV

Table 3. Parameters of the resonance doublets used for calculating the mass loss rate. The parameters for the N V, Si IV and C IV doublets were taken from Bianchi et al. (1986). For the other lines the parameters were obtained from the best fit profiles shown in figure 3. The table lists also the laboratory wavelengths λ_0 and oscillator strengths f of the corresponding transitions taken from Snow and Morton (1976).

Ion	λ_0 [nm]	f	v_∞ [km/s]	τ_{tot}	γ
S VI	93.3	0.426	1550	80	3
S VI	94.5	0.210			
O VI	103.2	0.130	1970	115	3
O VI	103.8	0.065			
P V	111.8	0.495	1550	2.5	1.5
P V	112.8	0.245			
N V	123.9	0.152	1940	150	6
N V	124.3	0.076			
Si IV	139.4	0.528	1520	0.6	1
Si IV	140.3	0.262			
C IV	154.8	0.194	1900	1500	3.5
C IV	155.1	0.097			

(154.8 nm, 155.1 nm) analysed by them with the same method using the same velocity and optical depth laws. Table 3 contains additionally the laboratory wavelengths and oscillator strengths for the corresponding transitions, taken from Snow and Morton (1976), which were used for the calculation of the mass loss rate (see below).

We computed the mass loss rate from (Bianchi et al. 1986)

$$\frac{\dot{M}}{[M_\odot/\text{yr}]} = 8.9 \cdot 10^{-24} \frac{R_* v_\infty^2 \tau_{\text{tot}}}{f A_\beta \lambda_0} \left(\int_{w_0}^1 \frac{g_{\beta,i}}{x^2 w} \frac{dw}{dx} dx \right)^{-1}$$

where the stellar radius R_* is in R_\odot , the terminal velocity v_∞ in km/s, the laboratory wavelength λ_0 of the transition in nm, and where f denotes the oscillator strength of the transition (see table 3). A_β is the abundance of the element β by number with respect to hydrogen. Castor et al. (1981) claim that there are no significant differences between the abundances in the central star of NGC 6543 and those found in the sun. This has been confirmed by subsequent work, the most important being the one by Aller and Czyzak (1983). Therefore we assumed as abundances the solar values $A_S = 1.7 \cdot 10^{-5}$, $A_O = 6.6 \cdot 10^{-4}$, $A_P = 3.3 \cdot 10^{-7}$, $A_N = 9.1 \cdot 10^{-5}$, $A_{\text{Si}} = 3.3 \cdot 10^{-5}$ and $A_C = 3.3 \cdot 10^{-4}$ from Allen (1973). In order to evaluate the mass loss rate using the equation above one has to determine the ionization fraction $g_{\beta,i} = n_{\beta,i}/n_\beta$ for each ion β^{+i} as a function of the distance from the stellar surface. We solved the ionization equilibrium in the wind for a grid of 1 000 points between $x=1$ and $x=100$ and used the ionization fractions obtained in this way for the calculation of the integral in the equation above. The ionization equilibrium was computed at each point in the wind using a modified form of formula 6 from Bernacca and Bianchi (1979), which considered in its original version photoionization, radiative recombination onto the ground level and geometrical dilution of the central star's radiation. Since collisional ionization is not negligible for electron densities greater than approximately 10^{14} cm^{-3} we considered additionally collisional ionization. Aldrovandi and

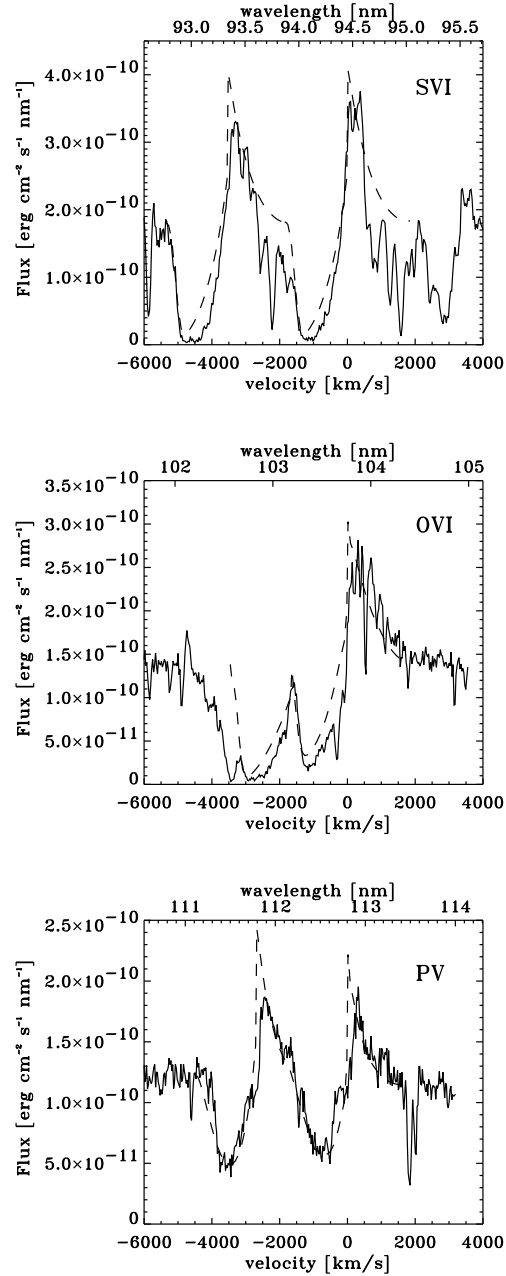


Fig. 3. Observed P-Cygni line profiles of the S VI, O VI and PV resonance doublets, smoothed by a Gaussian curve with a FWHM of 0.01 nm (solid lines). Superimposed are theoretical line profiles calculated by the escape probability method (dashed lines).

Péquignot (1973) have published radiative and dielectronic recombination coefficients for a number of different ions. They quote for each ion a critical temperature below which dielectronic recombinations are negligible. For the ions considered here (O VI, P V, S VI, N V, Si IV and C IV) these critical temperatures are all greater than 150 000 K. Since we assumed for the computation of the ionization equilibrium an electron temperature of 50 000 K in the wind we have neglected dielectronic recombinations in our calculations.

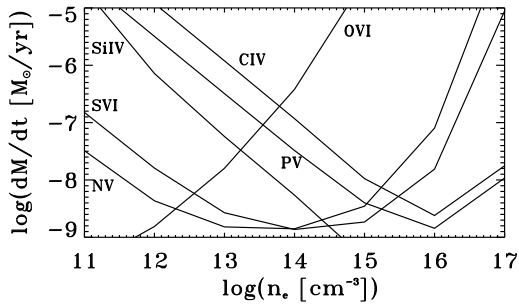


Fig. 4. Stellar mass loss rate as a function of the electron density at the base of the expanding stellar atmosphere.

Under equilibrium conditions of ionization and recombination the ionization fractions depend on the electron density, the radiation temperature T_{rad} and the electron temperature T_e in the wind. If the wind satisfies the assumptions that enter in the equations used, the same value of the electron density at the base of the wind should result from the computations for the different lines. The problem is the choice of the radiation and the electron temperature. The radiation temperature might reasonably be taken close to the effective temperature of the central star, but it is uncertain which would be the most appropriate electron temperature to use. Calculations for NGC 6543 made by Olson and reported by Castor et al. (1981) gave a good fit to their observed ionization fractions of O IV, O V and Si IV with $T_{\text{rad}} = 37\,000\text{ K}$ and $T_e = 170\,000\text{ K}$. However the high electron temperature caused other problems discussed by Castor et al. (1981) with their observations and they excluded therefore this 'warm wind' model for NGC 6543. We assumed a wind model with $T_{\text{rad}} = T_e = T_* = 50\,000\text{ K}$.

Using these temperature values for the calculation of the ionization balance we obtained for the ionization fractions of the different ions in the wind the following mean values: 0.035 for P V, 10^{-13} for O VI, $3 \cdot 10^{-4}$ for S VI, 0.038 for C IV, $2 \cdot 10^{-5}$ for N V and 0.68 for Si IV.

In Fig. 4 the mass loss rate is plotted for each doublet as a function of the electron density at the base of the wind. We considered additionally to the resonance doublets of S VI, O VI and P V observed by ORFEUS, the resonance doublets of N V, Si IV and CIV observed by IUE, which were already analysed by Bianchi et al. (1986). For these three latter lines we made a reanalysis of the mass loss rate using the stellar parameters from Sect. 3.1 with the additional consideration of collisional ionization in the determination of the ionization fractions. The profile parameters used for the computation of the mass loss rate are summarized in table 3. As a first estimate for the mass loss rate we find $\dot{M} = 7.1 \cdot 10^{-9} M_{\odot}/\text{yr}$.

This value can only be regarded as a lower limit to the real mass loss rate, because the observed profiles of S VI, O VI, N V and CIV are strongly saturated. The uncertainties in the derived electron density at the base of the wind and the mass loss rate are quite large. The values scatter between $1.8 \cdot 10^{12}\text{ cm}^{-3}$ and $3.2 \cdot 10^{15}\text{ cm}^{-3}$ for the electron density and between $1.3 \cdot 10^{-9} M_{\odot}/\text{yr}$ and $2 \cdot 10^{-7} M_{\odot}/\text{yr}$ for the mass

loss rate. These large uncertainties probably arise from the fact that our calculations of the ionization equilibrium do not predict an appreciable abundance of O VI in the wind. Also the assumption of electron temperatures in the wind greater than $50\,000\text{ K}$ could not solve this problem. We would like to mention explicitly, that this is a general limitation of the theory used here.

Pauldrach et al. (1988) have shown, by means of detailed, multi-level NLTE calculations for the ionization and the excitation balance in stellar winds, which are done simultaneously with the computation of the hydrodynamics of the winds, that high ionization species such as O VI can be explained by photoionization from excited levels in a wind which is in radiative equilibrium with the photosphere. But this is far beyond the scope of this paper. If one ignores O VI in figure 4 the electron density at the base of the wind and the mass loss rate are more clearly defined. One finds then for the mean value of the mass loss rate a lower limit of $2.8 \cdot 10^{-9} M_{\odot}/\text{yr}$ and for the electron density at the base of the wind a mean value of $5.6 \cdot 10^{14}\text{ cm}^{-3}$.

A comparison of our determination of the mass loss rate with other previous direct empirical ones show that the most extreme values differ by a factor of 1000 (table 1). The very large scatter of the mass loss rate reflect mainly the uncertainties of the ionization calculations. The differences also originate partly from the methods used to analyze the observed profiles and partly from the different stellar parameters adopted by the various authors.

If one calculates the expected mass loss rate and terminal velocity for a radiation driven wind using the approximate radiation driven wind theory by Kudritzki et al. (1989) one obtains for the stellar parameters $M_* = 0.62 M_{\odot}$, $T_* = 50\,000\text{ K}$, $R_* = 0.73 R_{\odot}$ and $L_* = 3\,030 L_{\odot}$, which we have used for the determination of the mass loss rate, a mass loss rate of $4.2 \cdot 10^{-9} M_{\odot}/\text{yr}$ and a terminal velocity of $1\,899\text{ km/s}$. These values are in good agreement with our determinations from the observations.

Hydrodynamical simulations for the shaping of planetary nebulae, which assume the interaction of a fast, tenuous wind originating from the central star with the slowly expanding material expelled during the asymptotic giant branch evolution of the progenitor star, predict hot, low density gas in the interior of the nebular shell. A search for coronal emission and absorption lines in the ORFEUS spectrum of the central star of NGC 6543 yields no definitive evidence for such a hot bubble (Zweigle 1996).

4. Summary

From the comparison of the stellar continuum with model atmospheres we obtained a stellar temperature of $50\,000\text{ K}$ for the central star of NGC 6543 and an estimate for its distance of 1310 pc . Furthermore we have analysed the prominent P-Cygni line profiles of the resonance doublets of S VI, O VI and P V in the ORFEUS far ultraviolet spectrum and calculated the stellar mass loss rate including the N V, Si IV and CIV lines in the IUE wavelength range. The derived lower limit for the mass

loss rate of $2.8 \cdot 10^{-9} M_{\odot}/\text{yr}$ is compatible within a factor of two with the expected mass loss rate for a hot star with parameters $M_{\star} = 0.62 M_{\odot}$, $L_{\star} = 3\,030 L_{\odot}$ and $T_{\star} = 50\,000\text{ K}$ using the approximate radiation driven wind theory by Kudritzki et al. (1989).

Acknowledgements. The ORFEUS-SPAS mission could not have succeeded without the dedicated work of the hardware groups at Tübingen, Heidelberg and Berkeley and the effort and efficient support by NASA, DARA, DASA and Kayser-Threde. This research was supported by the BMFT/BMBF (DARA) through grant 01 OS 8501 and NASA grant NAG 5-696. This research has made use of the Simbad database, operated at CDS, Strasbourg, France. We thank Dr. R. P. Kudritzki for making available to us a version of his program for calculating the terminal wind velocity and the stellar mass loss rate for hot stars as function of the stellar mass, radius and temperature. We are grateful to the referee Dr. M. Perinotto for his valuable comments for improving the paper.

References

- Acker A., Marcout J., Ochsenbein F., Stenholm B., Tylenda R., 1992, The Strasbourg-ESO catalogue of galactic planetary nebulae
- Aldrovandi S.M.V., Péquignot D., 1973, *A&A* 25, 137
- Aller L.H., Czyzak J.C., 1983, *ApJS* 51, 211
- Allen C.W., 1973, *Astrophysical Quantities*, The Athlon Press University, London & Atlantic Highlands
- Balick B., Perinotto M., Maccioni A., Terzian Y., Hajian A., 1994, *ApJ* 424, 800
- Bernacca P.L., Bianchi L., 1979, *A&A* 75, 61
- Bianchi L., Cerrato S., Grewing M., 1986, *A&A* 169, 227
- Boksenberg A., Carnochan D., Cahn J.H., Wyatt S.P., 1975, *MNRAS* 172, 395
- Bowers C.W., Blair W.P., Long K.S., Davidsen A.F., 1995, *ApJ* 444, 748
- Castor J.I., Lutz J.H., Seaton M.J., 1981, *MNRAS* 194, 547
- Clegg R.E.S., Middlemass D., 1987, *MNRAS* 228, 759
- Fruscione A., Drake J.J., Mc Donald K., Malina R.F., 1995, *ApJ* 441, 726
- Górny S.K., Stasińska G., Tylenda R., 1996, preprint, to appear in *A&A*
- Harrington J.P., Borkowski K.J., 1994, *BAAS* 26, 1469
- Hurwitz M., Bowyer S., 1991, in: *Extreme Ultraviolet Astronomy*, ed. R.F. Malina & S. Bowyer (New York; Pergamon), 437
- Hurwitz M., Bowyer S., 1995, *ApJ* 446, 812
- Hurwitz M., Bowyer S., 1996, *ApJ* 465, 296
- Hutsemékers D., Surdej J., 1987, *A&A* 173, 101
- Hutsemékers D., Surdej J., 1989, *A&A* 219, 237
- Kreysing H.C., Diesch C., Zweigle J., Staubert R., Grewing M., Hasinger G., 1992, *A&A* 264, 623
- Kudritzki R.P., Pauldrach A., Puls J., Abbott D.C., 1989, *A&A* 219, 205
- Savage B.D., Mathis J.S., 1979, *Ann. Rev. A&A* 17, 73
- Mendez R.H., Herrero A., Manchado A., 1990, *A&A* 229, 152
- Miranda L.F., Solf J., 1992, *A&A* 260, 397
- Morton, D.C. 1991, *ApJS* 77, 119
- Natta A., Pottasch S.R., Preite-Martinez A., 1980, *A&A* 84, 284
- Olson G.L., 1982, *ApJ* 255, 267
- Patriarchi P., Perinotto M., 1995, *A&AS* 110, 353
- Pauldrach A., Kudritzki R.P., Gabler R., Wagner A., 1988, in: *Mass Outflows from Stars and Galactic Nuclei*, ed. L. Bianchi & R. Gilmozzi (Dordrecht;Kluwer), 63
- Perinotto M., Cerruti-Sola M., Lamers H.J.G.L.M., 1989, *ApJ* 337, 382
- Polidan, R.S., Holberg J.B. 1985, in *IAU Symp. 111, Calibration of Fundamental Stellar Quantities*, ed. D.S. Hayes, L.E. Pasinetti, & A.G. Davis Philip (Dordrecht: Reidel), 479
- Raymond J.C., Mauche C.W., Bowyer S., Hurwitz M., 1995, *ApJ* 440, 331
- Savage B.D., Bohlin R.C., Drake J.F., Budich W., 1977, *ApJ* 216, 291
- Seaton M.J., 1979, *MNRAS* 187, P73
- Snow T.P.Jr., Morton D.C., 1976, *ApJS* 32, 429
- Zweigle J., 1996, PhD thesis, Universität Tübingen